ESC HEART FAILURE
ESC Heart Failure 2023; **10**: 578–593
Published online 11 November 2022 in Wiley Online Library (wileyonlinelibrary.com) **DOI:** 10.1002/ehf2.14169

ORIGINAL ARTICLE

Dapagliflozin reduces pulmonary vascular damage and susceptibility to atrial fibrillation in right heart disease

Chang Dai[1,2,3], Bin Kong[1,2,3], Wei Shuai[1,2,3], Zheng Xiao[1,2,3], Tianyou Qin[1,2,3], Jin Fang[1,2,3], Yang Gong[1,2,3], Jun Zhu[1,2,3], Qi Liu[1,2,3], Hui Fu[1,2,3], Hong Meng[1,2,3] and He Huang[1,2,3]*

[1]*Department of Cardiology, Renmin Hospital of Wuhan University, 238 Jiefang Road, 430060, Wuhan, Hubei, P.R. China;* [2]*Cardiovascular Research Institute of Wuhan University, Wuhan, Hubei, P.R. China; and* [3]*Hubei Key Laboratory of Cardiology, Wuhan, Hubei, P.R. China*

Abstract

Aims Sodium-glucose cotransporter 2 inhibitors (SGLT2is) have made considerable progress in the field of heart failure, but their application in arrhythmia remains to be in-depth. Right heart disease (RHD) often leads to right heart dysfunction and is associated with atrial fibrillation (AF). Here, we explored the possible electrophysiologic effect of dapagliflozin (a type of SGLT2is) in the development of AF in rats with RHD.

Methods and results Rats in the experimental group were intraperitoneally injected with a single dose of 60 mg/kg monocrotaline (MCT group, n = 32) on the first day of the experiment, whereas rats in the control group were injected with vehicle (CTL group, n = 32). Rats in the treatment subgroup were treated with dapagliflozin solution orally (MCT + DAPA and CTL + DAPA groups) for a total of 4 weeks, whereas rats in the rest of subgroups were given sterile drinking water. After 4 weeks, echocardiography demonstrated that MCT group rats developed obvious pulmonary arterial hypertension and right heart dysfunction. In addition, there were also obvious inflammatory infiltration, fibrosis, and muscularization in right atrial and pulmonary arteries. The P-wave duration (17.00 ± 0.53 ms, vs. 14.43 ± 0.57 ms in CTL; 14.00 ± 0.65 ms in CTL + DAPA; 14.57 ± 0.65 ms in MCT + DAPA; $P < 0.05$), RR interval (171.60 ± 1.48 ms, vs. 163.10 ± 1.10 ms in CTL; 163.30 ± 1.19 ms in CTL + DAPA; 163.10 ± 1.50 ms in MCT + DAPA; $P < 0.05$), Tpeak-Tend interval (65.93 ± 2.55 ms, vs. 49.55 ± 1.71 ms in CTL; 48.27 ± 3.08 ms in CTL + DAPA; $P < 0.05$), and corrected QT interval (200.90 ± 2.40 ms, vs. 160.00 ± 0.82 ms in CTL; 160.40 ± 1.36 ms in CTL + DAPA; 176.6 ± 1.57 ms in MCT + DAPA; $P < 0.01$) were significantly prolonged in the MCT group after 4 weeks, whereas P-wave amplitude (0.07 ± 0.0011 mV, vs. 0.14 ± 0.0009 mV in CTL; 0.14 ± 0.0011 mV in CTL + DAPA; 0.08 ± 0.0047 mV in MCT + DAPA; $P < 0.05$) and T-wave amplitude (0.04 ± 0.002 mV, vs. 0.13 ± 0.003 mV in CTL; 0.13 ± 0.003 mV in CTL + DAPA; $P < 0.01$) were decreased, and atrial 90% action potential duration (47.50 ± 0.93 ms, vs. 59.13 ± 2.1 ms in CTL; 59.75 ± 1.13 ms in CTL + DAPA; 60.63 ± 1.07 ms in MCT + DAPA; $P < 0.01$) and effective refractory periods (41.14 ± 0.88 ms, vs. 62.86 ± 0.99 ms in CTL; 63.14 ± 0.67 ms in CTL + DAPA; 54.86 ± 0.70 ms in MCT + DAPA; $P < 0.01$) were shortened. Importantly, the inducibility rate (80%, vs. 0% in CTL; 10% in CTL + DAPA; 40% in MCT + DAPA; $P < 0.05$) and duration of AF (30.85 ± 22.90 s, vs. 0 ± 0 s in CTL; 0.24 ± 0.76 s in CTL + DAPA; 5.08 ± 7.92 s in MCT + DAPA; $P < 0.05$) were significantly increased, whereas the expression levels of cardiac ion channels and calcium-handling proteins such as potassium/calcium channels and calmodulin were decreased. Mechanistically, 'NACHT, LRR, and PYD domain-containing protein 3' inflammasome-related pathway was significantly activated in the MCT group. Nevertheless, in the MCT + DAPA group, the above abnormalities were significantly improved.

Conclusions Dapagliflozin reduces pulmonary vascular damage and right heart dysfunction, as well as the susceptibility to AF in RHD rats.

Keywords Dapagliflozin; Atrial fibrillation; Right heart disease; Pulmonary arterial hypertension; Monocrotaline; Electrocardiography

Received: 25 March 2022; Revised: 13 August 2022; Accepted: 15 September 2022
**Correspondence to: He Huang, FACC, FESC, FEHRA, FHRS, FAPHRS, Department of Cardiology, Renmin Hospital of Wuhan University, 238 Jiefang Road, Wuhan 430060, Hubei, P.R. China. Tel: 86-27-88041911; Fax: +86 27 88070797. Email: huanghe1977@whu.edu.cn*
Chang Dai and Bin Kong contributed equally to the study.

Introduction

Sodium-glucose cotransporter 2 inhibitors (SGLT2is) are hailed as the statins of the 21st century.[1] Since the initial put into use in blood glucose management by increasing glucose excretion in urine independent of insulin secretion,[2] its clinical application has been expanded from secondary prevention of cardiovascular diseases to the primary prevention. Several ground-breaking studies have demonstrated that SGLT2is can reduce the risk of cardiovascular death or heart failure (HF) deterioration in patients with or without diabetes, and they can also reduce the all-cause mortality risk in HF patients by up to 17%.[2–5] Therefore, SGLT2is have become the new cornerstone in the field of HF prevention and treatment.[6] Recent real-world data suggested that SGLT2is can reduce the risk of atrial arrhythmia in patients with type 2 diabetes mellitus or HF.[7,8] Therefore, based on the observed promising clinical antiarrhythmic effects of SGLT2is on atrial arrhythmias in the real world, it is necessary to further explore the potential mechanism and effect of SGLT2is in a more controlled laboratory experiments setting.

Atrial fibrillation (AF) is a common type of atrial arrhythmia, which is mainly initiated by abnormal electrical activity of atria adjacent to thoracic veins (including pulmonary vein, vena cava, coronary sinus, and ligament of Marshall), and its trigger origins are often multi-source.[9] Studies have confirmed that some AF could arise from right atrium and characterize the right atrial ectopic initiation and right-to-left dominant frequency gradients.[10] Moreover, the mapping and ablation of complex fragmentation potentials not only for left atrium and pulmonary veins but also for both left and right atria can improve the success rate in patients with permanent and persistent AF,[11] suggesting that AF triggered by right atrium may be underestimated compared with left atrial AF and deserves further attention. Not only that, but current studies have confirmed that in addition to left heart-related diseases, right heart disease (RHD) can also increase the risk of AF.[12–14] Therefore, it is necessary to further clarify the pathogenesis of AF, so as to increase the comprehensive understanding of AF and provide new ideas for the treatment of AF. In addition to the secondary right heart dysfunction caused by ischaemia, cardiomyopathy, or congenital cardiac structural abnormalities, the right heart dysfunction due to pulmonary vascular remodelling is also one of the RHD associated with increased risk of AF,[12] and its central process to the pathogenesis may be related to the expansion or extension of right atrium caused by the pulmonary arterial hypertension (PAH), which is induced by increased right atrial afterload, tricuspid regurgitation, and right atrial hypertrophy.[13,15] Considering that SGLT2is have a therapeutic effect on patients with HF and can significantly reduce the risk of atrial arrhythmia (including but not limited to AF) in patients with HF, as a representative type of SGLT2is, the therapeutic effect of dapagliflozin on right heart dysfunction and RHD-induced AF is also expected.

Materials and methods

Animals and animal model

All animal experimental procedures in our study were carried out in compliance with the Guide for the Care and Use of Laboratory Animals published by the US National Institutes of Health (NIH Publication, revised in 2011) and approved by the Animal Care and Use Committee of Renmin Hospital of Wuhan University (Protocol No. 20190429).

Sixty-four adult male Sprague Dawley (SD) rats (300–350 g, 8–10 weeks) were provided by the Hubei Provincial Center for Disease Control and Prevention (Hubei, China). The rats were conditioned in-house for 1 week after arrival with sterile drinking water and commercial diet available at will. Rats were housed in conditions under temperature of 22 ± 2°C and a 12:12 h light/dark cycle with free access to food and water ad libitum.

Rats were randomly assigned to control (CTL) group or monocrotaline (MCT) group (n = 32 per group) and raised for 4 weeks (28 days). Rats in the MCT group experienced a single intraperitoneal dose (60 mg/kg) of MCT, which will eventually lead to the occurrence of pulmonary vascular remodelling after around 21 days,[15] and rats in the CTL group were intraperitoneally injected with the same volume of dimethyl sulfoxide (DMSO, 1% final concentration). Each group mentioned above was randomly divided into vehicle-treated and dapagliflozin-treated subgroups. The SGLT2i, dapagliflozin, was dissolved in sterile drinking water at a final concentration of 60 mg/L for free use by dapagliflozin-treated subgroup rats during the 4 weeks of the experiment,[16] whereas rats in the vehicle-treated subgroup were fed with normal sterile drinking water. The daily water consumption of an adult male SD rat was calculated as 10 mL/100 g, and the actual daily water consumption was determined based on their measured body weight. We provided rats with the corresponding volume of drinking solution according to the above calculation method.

On Day 28 post-MCT, echocardiography was performed under inhaled anaesthesia (2% isoflurane/100% oxygen), and then the rats were sacrificed to remove the heart and Langendorff perfusion or dissection for histological/biochemical studies was performed. Right ventricular hypertrophy index (RVHI) was assessed based on right ventricular mass/(left ventricular mass + interventricular septum mass).

DOI: 10.1002/ehf2.14169

Blood glucose measurement

Blood samples were collected from the tail vein of rats at fixed time every week, and the blood glucose was measured by glucometer (ACCU-CHEK, Roche Diabetes Care GmbH).

Haemodynamic measurement

The blood pressure was measured while the rats were awake and unstimulated at the end of the fourth week through blood pressure metre (BP-2010A, Softron Beijing Biotechnology).

Echocardiography

Cardiac structure and function were assessed by echocardiography at the end of the fourth week. Echocardiography was carried out using the VINNO 6VET ultrasound system (Vinno Technology, Suzhou, Jiangsu, China) equipped with 18 MHz linear array transducer (Vinno Technology) after rats were placed in the supine position on an electrical heating pad under anaesthesia (2% isoflurane/100% oxygen). In addition to the measurement of structural and functional indexes of the left and right heart, pulmonary vascular remodelling and pulmonary arterial pressure changes caused by MCT were assessed by pulmonary arterial flow spectrum acceleration time (AT), pulmonary arterial flow spectrum ejection time (ET), the ratio of AT/ET, and left ventricular eccentricity index (LVEI). The averaged echocardiographic parameters were collected from consistently three to five cardiac cycles. The investigator performing the measurements was blinded to the treatment allocation.

Histology and histochemistry analysis

The rat hearts were fixed with 4% paraformaldehyde overnight, then embedded in paraffin, and sliced into 5 μm sections. Haematoxylin–eosin (H&E) staining, Masson staining, and immunohistochemistry were performed. Detailed procedures and methods are provided in the supporting information.

Quantitative real-time PCR and western blot

Total cardiac RNA and proteins were extracted from the atrial tissues. Detailed procedures and methods are provided in the supporting information.

Electrocardiographic analysis

Rats were anaesthetized with inhaled isoflurane (2% isoflurane/100% oxygen). Then, the two subcutaneous leads were positioned approximately on electrocardiograph (ECG) limb lead II. Common electrophysiological parameters [the P-wave duration, QRS duration, P/T-wave amplitude, RR interval, PR interval, Tpeak-Tend interval, and corrected QT (QTc) interval] were analysed off-line using LabChart 7 Pro (AD Instruments, Sydney, Australia). ECG waveforms averaged over four consecutive beats were used for analyses.

Electrophysiological studies of isolated perfused hearts

Langendorff-perfused hearts were prepared according to published methods.[17] Detailed electrical stimulation and measurement methods are provided in the supporting information.

Drugs and reagents

Dapagliflozin was purchased from AstraZeneca AB (Mondale, Sweden). MCT (98% purity, C835791) was obtained from Macklin Biochemical Co., Ltd (Shanghai, China). Detailed reagents are provided in the supporting information.

Statistical analysis

Statistical analyses were performed by Statistical Product and Service Solutions (SPSS) and GraphPad Prism software. Continuous variables are presented as means ± standard error of the mean (SEM). For all analyses, sample size is reported in the figure legends. For data with a Gaussian distribution, two-group analysis used unpaired Student's *t*-test (equal variance) or unpaired Student's *t*-test with Welch's correction (unequal variance). Comparisons of multiple groups were performed using either one-way or two-way ANOVA (as appropriate). Post hoc multiple comparisons testing used a Tukey test. For data with a non-Gaussian distribution, we performed a non-parametric statistical analysis using the Mann–Whitney *U* test for comparisons between two groups or the Kruskal–Wallis test for multiple comparisons. A P value < 0.05 was considered statistically significant.

Results

General status and blood glucose changes during the period of pulmonary vascular remodelling in rats

In this study, we observed that during the pathological process of pulmonary vascular remodelling in the MCT group, the mucosa around the lips, tongue, nose, and limbs of rats gradually appeared cyanosis, and their hair became upright. In addition, the rats suffered from breathlessness after exercises and they also showed low foraging desire. However, in the MCT + DAPA group, the hypoxia and decreased exercise tolerance caused by this kind of pulmonary vascular remodelling-associated RHD were significantly relieved. As the experiment time goes on, the body weight gain of rats in the MCT group was slower than that in the CTL group, which was consistent with the previous research trend of establishing PAH rat model by MCT.[18] Meanwhile, the body weight gain in the CTL + DAPA group was also lower than that in the other groups (*Figure 1A*), which may be related to the hypoglycaemic effect of dapagliflozin. In addition, the overall average blood glucose level in the CTL, CTL + DAPA, MCT, and MCT + DAPA groups was 7.49 ± 0.55, 7.24 ± 0.76, 6.78 ± 0.67, and 7.27 ± 0.61 mmol/L, respectively, suggesting that the blood glucose level in the MCT group was lower than that in the other groups ($P < 0.01$) (*Figure 1B*). In the MCT group, due to the toxic effect of MCT, the overall health status of rats was poor and the foraging quantity was reduced, which may be one of the reasons for the difference in body weight compared with the CTL group, and this is also consistent with the results of a statistically significant decrease in overall blood glucose. In the CTL + DAPA group and the MCT + DAPA group, although the overall decrease of blood glucose level was not significant, the body weight gain was conversely the smallest, which may be related to the mobilization of non-sugar energy substances such as fat and protein in various parts of the body into blood glucose to compensate for the increased urinary glucose excretion caused by dapagliflozin. Besides, it is recognized that changes in body weight are not just about blood glucose level. In many metabolic diseases such as diabetes, blood glucose level is not representative in assessing whether one is fat or thin. Not to mention this study only assessed random blood glucose in the same period of each week. Therefore, the mechanism of how dapagliflozin affects metabolism requires more dimensions of evaluation parameters to go deep.

Dapagliflozin can improve cardiac structural remodelling, cardiac function, and haemodynamic disorders secondary to pulmonary vascular remodelling

In previous studies, invasive haemodynamic measurements have confirmed that the right ventricular systolic pressure was up to more than 40 mmHg in rats induced by MCT after 21 days, which was significantly higher than 20–30 mmHg in the CTL group,[15] and met the modelling standard of PAH. Besides, research has also suggested that the non-invasive evaluation of pulmonary arterial pressure by transthoracic echocardiography (TTE) correlates well with invasive measurements, and it is a reliable method for the assessment of pulmonary circulation.[19,20] Moreover, TTE is very suitable for the non-invasive diagnosis of PAH and has an acceptable specificity and sensitivity in detecting PAH.[21] Therefore, we

Figure 1 General status and blood glucose changes during the period of pulmonary vascular remodelling ($n = 10$). (A) Body weight in each group. (B) Overall blood glucose changes in each group. Data are presented as mean ± standard error of the mean (SEM). *$P < 0.05$, **$P < 0.01$, ***$P < 0.001$, ****$P < 0.0001$. The groups without statistical difference were not labelled. CTL, control; DAPA, dapagliflozin; MCT, monocrotaline.

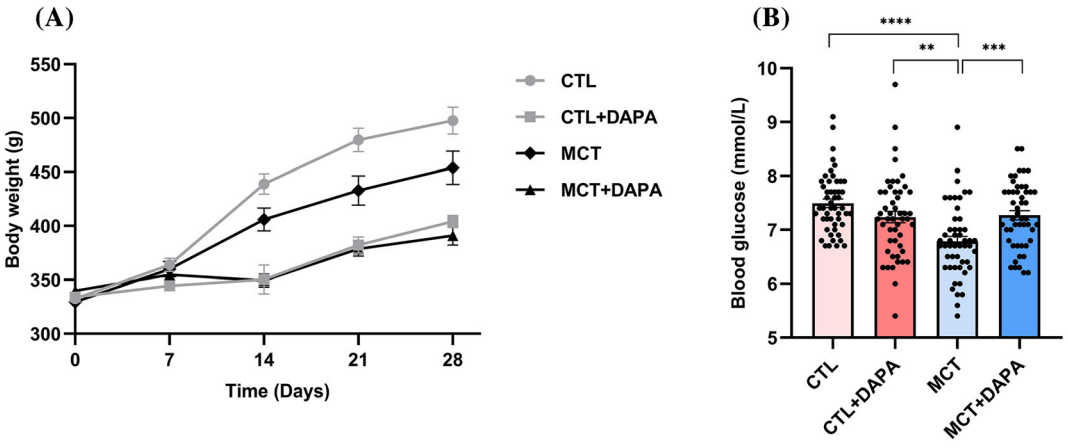

DOI: 10.1002/ehf2.14169

comprehensively evaluated the cardiac structure and function through TTE and blood pressure metre.

In this research, after 4 weeks, there was no significant difference in heart rate (HR) among groups (365.50 ± 12.89 b.p.m. in the CTL group; 370.40 ± 14.55 b.p.m. in the CTL + DAPA group; 411.30 ± 16.03 b.p.m. in the MCT group; 365.80 ± 11.63 b.p.m. in the MCT + DAPA group; $P > 0.05$) (*Figure 2A*), but the systolic blood pressure in the CTL group (142.10 ± 2.02 mmHg, vs. 124.00 ± 2.72 mmHg in the CTL + DAPA group, $P < 0.01$; vs. 123.60 ± 1.95 mmHg in the MCT group, $P < 0.01$; vs. 133.20 ± 3.25 mmHg in the MCT + DAPA group, $P > 0.05$) was ~19–21 mmHg higher than the MCT group and the CTL + DAPA group, whereas the diastolic blood pressure in the CTL group (115.70 ± 2.38 mmHg, vs. 98.28 ± 2.47 mmHg in the CTL + DAPA group; 96.23 ± 2.45 mmHg in the MCT group; 105.90 ± 2.97 mmHg in the MCT + DAPA group; $P < 0.05$) was ~10–19 mmHg higher than the other groups. Compared with the CTL group, the MCT + DAPA group only showed significant decrease in diastolic blood pressure (*Figure 2B,C*). Beyond that, in the MCT group, the pulmonary vessels were significantly remodelled, and the right heart function (including atrium and ventricle) was also significantly changed (*Table 1*). Generally, among the parameters measured by echocardiography, AT and AT/ET are negatively correlated with pulmonary arterial pressure, whereas the LVEI is positively correlated with pulmonary arterial pressure and right ventricular afterload. Although the pulmonary arterial pressure could not be directly estimated, the parameters mentioned above and related peak blood flow velocity of tricuspid valve orifice haemodynamic parameters all changed significantly in the MCT group ($P < 0.05$) (*Table 1*). Moreover, it was obvious from the pulmonary arterial spectrum and apical four-chamber section (*Figure 2D*) that the pulmonary arterial flow spectrum in the MCT group presented a narrow triangle with the peak moving forward, and the right heart chambers (including right atrium and right ventricle) were significantly dilated compared with the left heart chambers, suggesting that the model of RHD caused by PAH is successful. In addition, the structural diameters, tricuspid annular plane systolic excursion (TAPSE), and other parameters related to right heart function also showed significant abnormal changes (*Table 1*). Importantly, there was no significant difference in left heart function and structural parameters among groups. Interestingly, almost all haemodynamic disorders and structural abnormalities related to right heart were partially or completely reversed through the treatment of dapagliflozin and even returned to the state of no statistical difference with the CTL group.

In addition to non-invasive TTE and haemodynamic examination, we also measured the parameters of isolated heart. The results showed that the heart weight to tibia length (HW/TL) ratio (27.01 ± 1.23 mg/mm, vs. 22.49 ± 0.31 mg/mm in the CTL group; 22.75 ± 0.80 mg/mm in the CTL + DAPA group; 22.69 ± 1.16 mg/mm in the MCT + DAPA group; $P < 0.05$) and RVHI (0.37 ± 0.01, vs. 0.27 ± 0.02 in the CTL group; 0.28 ± 0.01 in the CTL + DAPA group; 0.29 ± 0.02 in the MCT + DAPA group; $P < 0.01$) were significantly increased in the MCT group (*Figure 2E,F*), which also suggested that the increase of afterload caused by pulmonary vascular remodelling will eventually lead to the secondary structural changes of right heart. Similarly, these changes could be reversed in the MCT + DAPA group.

Dapagliflozin can ameliorate the pathological process of pulmonary vascular remodelling, atrial fibrosis, and inflammatory infiltration

After 4 weeks, we observed that the lungs in the MCT group were grey with uneven surface, poor elasticity, and multi-focus haemorrhage spots. Meanwhile, the right heart also appeared significant hypertrophy in the MCT group. Furthermore, the histopathological examination of hearts and pulmonary arteries (*Figure 3A,B*) revealed obvious hypertrophy and structural disorder of the cardiomyocytes in the MCT group under light microscope, whereas the lumens of middle or small pulmonary arteries were significantly narrowed and partially occluded. Besides, the medial membrane was thickened and a large number of inflammatory cells were infiltrated in the tissue space, leading to the disorder of proliferation and arrangement of collagen fibres. Masson staining showed that collagen volume fraction (CVF) of pulmonary arteries (19.14 ± 1.20%, vs. 4.28 ± 0.35% in the CTL group; 4.80 ± 0.84% in the CTL + DAPA group; 8.71 ± 0.62% in the MCT + DAPA group; $P < 0.05$) and right atria (8.40 ± 0.62%, vs. 1.60 ± 0.40% in the CTL group; 1.55 ± 0.31% in the CTL + DAPA group; 6.21 ± 0.22% in the MCT + DAPA group; $P < 0.05$) in the MCT group were significantly higher than those in the CTL and CTL + DAPA groups but presented a relatively less increase compared with the MCT + DAPA group (*Figure 3C,D*). In addition, alpha-smooth muscle actin (α-SMA) immunohistochemistry also confirmed a significant increase in pulmonary fibrosis and pulmonary arterial muscularization in the MCT group (15.71 ± 0.55%, vs. 4.36 ± 0.12% in the CTL group; 2.94 ± 0.40% in the CTL + DAPA group; 11.16 ± 0.80% in the MCT + DAPA group; $P < 0.05$), and these pathological changes could be significantly improved with the treatment of dapagliflozin (*Figure 3E*).

Dapagliflozin can alleviate cardiac electrical remodelling and reduce susceptibility to atrial fibrillation induced by secondary right heart dysfunction

According to the structural and functional studies above, the right atrium of rats in the MCT group experienced compensatory hypertrophy and dilation during the process of

Figure 2 Dapagliflozin can improve cardiac structural remodelling, improve cardiac function, and balance haemodynamic disorders during pulmonary vascular remodelling (n = 10). (A) Heart rate in each group. (B) Systolic pressure in each group. (C) Diastolic pressure in each group. (D) Representative pulmonary arterial spectrum and apical four-chamber view in each group. (E) HW/TL ratio in each group. (F) RVHI in each group. Data are presented as mean ± standard error of the mean (SEM). *$P < 0.05$, **$P < 0.01$, ***$P < 0.001$, ****$P < 0.0001$. The groups without statistical difference were not labelled. CTL, control; DAPA, dapagliflozin; HW/TL, heart weight to tibia length; MCT, monocrotaline; RVHI, right ventricular hypertrophy index.

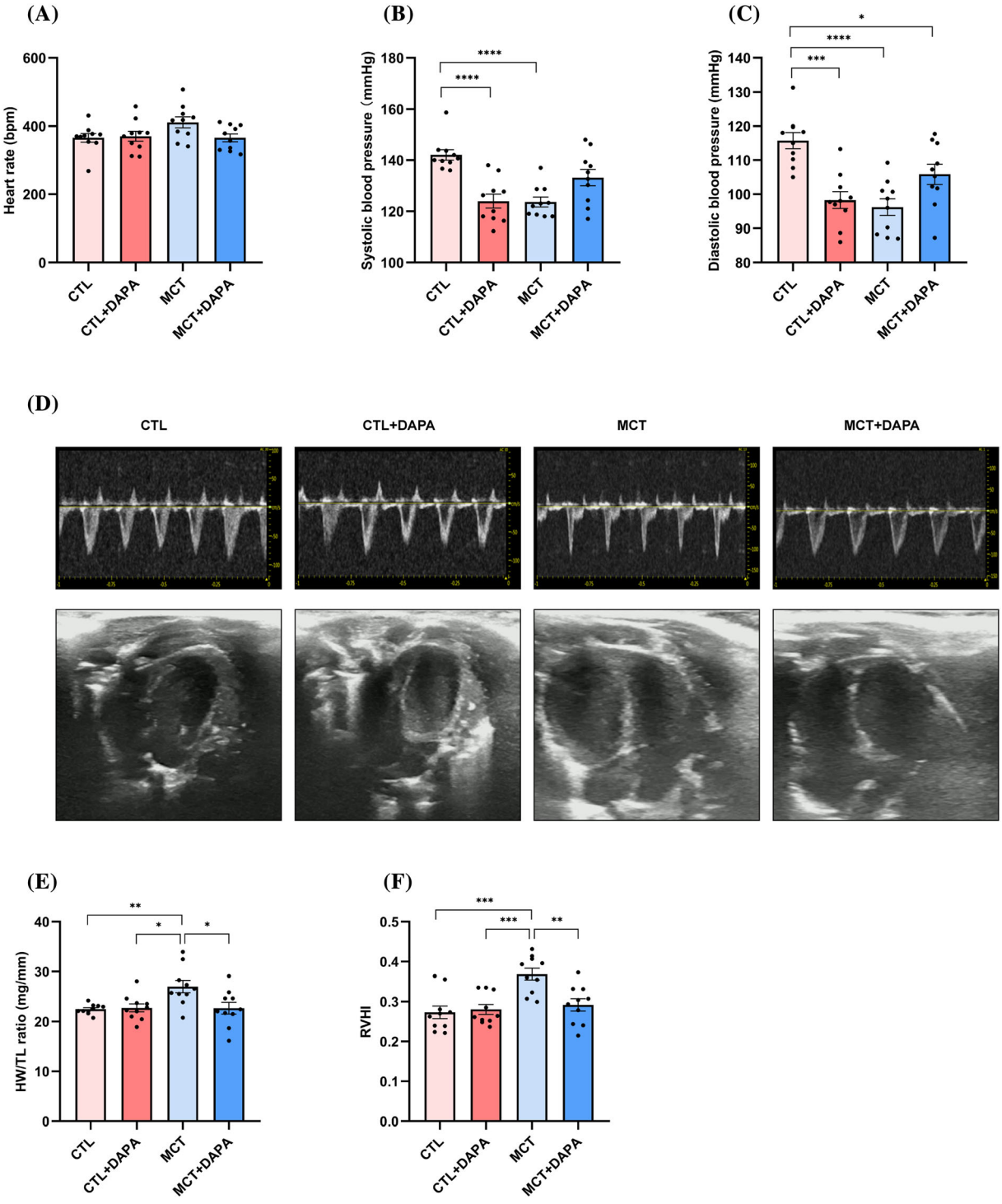

DOI: 10.1002/ehf2.14169

Table 1 The characteristics of cardiac function measured by echocardiography

		Control		MCT	
		Vehicle	DAPA	Vehicle	DAPA
HR (b.p.m.)		365.54 ± 40.76	370.4 ± 46.02	411.33 ± 50.68	365.77 ± 36.77
LVEF (%)		78.32 ± 1.64	80.93 ± 1.5	74.96 ± 6.03	76.11 ± 7.97
LVFS (%)		42.18 ± 1.58	44.44 ± 1.57	39.25 ± 5.37	40.67 ± 6.91
LVEDD (mm)		7.92 ± 0.76	7.04 ± 0.54	7.09 ± 0.62	7.12 ± 1.16
LVESD (mm)		4.35 ± 0.75	3.91 ± 0.34	4.08 ± 0.86	4.15 ± 1.09
LVEDV (mL)		1.11 ± 0.26	0.8 ± 0.18	0.82 ± 0.22	0.91 ± 0.38
LVESV (mL)		0.24 ± 0.06	0.15 ± 0.04	0.18 ± 0.1	0.20 ± 0.15
LVPWd (mm)		1.97 ± 0.12	1.79 ± 0.2	2.04 ± 0.18	1.83 ± 0.18
LVPWs (mm)		3.1 ± 0.19	2.89 ± 0.29	2.86 ± 0.24	2.68 ± 0.24
LVEI		0.05 ± 0.02	0.03 ± 0.04	0.31 ± 0.07*,**	0.12 ± 0.11†
IVSd (mm)		1.88 ± 0.18	1.74 ± 0.24	1.88 ± 0.26**	1.76 ± 0.28†
IVSs (mm)		3.07 ± 0.43	2.8 ± 0.41	2.56 ± 0.44	2.63 ± 0.4*
RVFWTd (mm)		0.51 ± 0.09	0.43 ± 0.07	1.33 ± 0.39*,**	0.55 ± 0.2†
RVFWTs (mm)		0.83 ± 0.1	0.74 ± 0.11	1.78 ± 0.45*,**	0.89 ± 0.24†
RVD (mm)		3.93 ± 0.39	3.53 ± 0.48	5.16 ± 0.66*,**	4.22 ± 0.73†
RVLD (mm)		10.8 ± 0.77	10.11 ± 1.28	11.42 ± 0.71**	10.33 ± 1.1†
PAD (mm)		3.23 ± 0.09	3.17 ± 0.33	4.14 ± 0.23*,**	3.53 ± 0.33†
AT (ms)		33.17 ± 3.31	33 ± 4.36	19.25 ± 4.16*,**	27.83 ± 6.55**,†
ET (ms)		81.67 ± 5.43	90.29 ± 7.34	85.58 ± 4.87	91 ± 12.07
AT/ET		0.41 ± 0.03	0.36 ± 0.03	0.22 ± 0.04*,**	0.30 ± 0.06**,†
PA-VTI (mm)		62.87 ± 12.74	63.94 ± 5.45	45.56 ± 8.35*,**	55.87 ± 11.73
TAPSE (mm)		2.4 ± 0.18	2.31 ± 0.28	1.6 ± 0.3*,**	1.98 ± 0.39†
RVFAC (%)		44.34 ± 3.87	46.4 ± 7.01	26.81 ± 9.73*,**	38.26 ± 11.36†
RADd (mm)	Axial	3.94 ± 0.54	3.65 ± 0.99	5.64 ± 1.81*,**	3.95 ± 0.71†
	Transverse	3.72 ± 0.45	3.21 ± 0.41	5.32 ± 1.56*,**	3.89 ± 0.72†
RADs (mm)	Axial	5.81 ± 0.64	5.17 ± 0.51	7.53 ± 1.7*,**	5.76 ± 0.84†
	Transverse	5.02 ± 0.67	4.44 ± 0.29	6.46 ± 1.23*,**	4.99 ± 0.92†
LADd (mm)	Axial	4.24 ± 0.56	3.85 ± 0.58	5.54 ± 1.3*,**	4.83 ± 0.83
	Transverse	3.78 ± 1.55	3.09 ± 0.34	3.74 ± 0.62	3.66 ± 0.61
LADs (mm)	Axial	5.91 ± 0.81	5.29 ± 0.15	6.69 ± 1.17**	5.96 ± 0.75
	Transverse	4.44 ± 0.66	3.99 ± 0.63	4.5 ± 0.49	4.23 ± 0.38
LAD (mm)	Anteroposterior	4.26 ± 0.41	4.13 ± 0.26	5.7 ± 0.92*,**	4.45 ± 0.58†
Peak blood flow velocity (cm/s)					
TVO	E	59.17 ± 21.2	49.22 ± 14.93	82.76 ± 19.22**	58.28 ± 15.39†
	A	80.4 ± 6.5	70.14 ± 15.25	59.8 ± 32.87	71.7 ± 10.48
MVO	E	59.67 ± 21.57	70.06 ± 18.86	67.57 ± 22.55	72.44 ± 17.6
	A	64 ± 12.98	60.91 ± 8.45	66.01 ± 14.8	64.18 ± 8.34

AT, pulmonary arterial flow spectrum acceleration time; DAPA, dapagliflozin; ET, pulmonary arterial flow spectrum ejection time; HR, heart rate; IVSd, interventricular septum thickness at left ventricular diastole; IVSs, interventricular septum thickness at left ventricular systole; LAD, left atrial anteroposterior diameter; LADd, left atrial diameter at diastole; LADs, left atrial diameter at systole; LVEDD, left ventricular end-diastolic dimension; LVEDV, left ventricular end-diastolic volume; LVEF, left ventricular ejection fraction; LVEI, left ventricular eccentricity index; LVESD, left ventricular end-systolic dimension; LVESV, left ventricular end-systolic volume; LVFS, left ventricular fraction shortening; LVPWd, left ventricular posterior wall thickness at end-diastole; LVPWs, left ventricular posterior wall thickness at end-systole; MCT, monocrotaline; MVO, mitral valve orifice; PAD, pulmonary arterial diameter; PA-VTI, pulmonary arterial spectrum velocity time integral; RADd, right atrial diameter at diastole; RADs, right atrial diameter at systole; RVD, right ventricular basal diameter; RVFAC, right ventricular fractional area change; RVFWTd, right ventricular free wall thickness at diastole; RVFWTs, right ventricular free wall thickness at systole; RVLD, right ventricular long diameter at end-diastole; TAPSE, tricuspid annular plane systolic excursion; TVO, tricuspid valve orifice.

n = 6–12 for each group. Data are presented as mean ± standard error of the mean (SEM).

*$P < 0.05$ vs. CTL group.

**$P < 0.05$ vs. CTL + DAPA group.

†$P < 0.05$ vs. MCT group.

pulmonary vascular remodelling, and the right heart function also declined accordingly. In this case, we calculated the electrophysiological data. In the MCT group and the MCT + DAPA group, T wave was low (T-wave amplitude: 0.04 ± 0.002 mV in the MCT group or 0.06 ± 0.006 mV in the MCT + DAPA group, vs. 0.13 ± 0.003 mV in the CTL group; 0.13 ± 0.003 mV in the CTL + DAPA group; $P < 0.01$) and flat (Tpeak-Tend interval: 65.93 ± 2.55 ms in the MCT group or 58.90 ± 1.36 ms in the MCT + DAPA group, vs. 49.55 ± 1.71 ms in the CTL group; 48.27 ± 3.08 ms in the CTL + DAPA group; $P < 0.05$) (*Figure 4A,E,F*). Compared with the CTL group and the CTL + DAPA group, the P-wave duration (17.00 ± 0.53 ms, vs. 14.43 ± 0.57 ms in the CTL group; 14.00 ± 0.65 ms in the CTL + DAPA group; 14.57 ± 0.65 ms in the MCT + DAPA group; $P < 0.05$), RR interval (171.60 ± 1.48 ms, vs. 163.10 ± 1.10 ms in the CTL group; 163.30 ± 1.19 ms in the CTL + DAPA group; 163.10 ± 1.50 ms in the MCT + DAPA group; $P < 0.05$), and QTc interval (200.90 ± 2.40 ms, vs. 160.00 ± 0.82 ms in the

Figure 3 Dapagliflozin can ameliorate the pathological process of pulmonary vascular remodelling, atrial fibrosis, and inflammatory infiltration (n = 3). (A) Representative images of H&E, Masson, and immunocytochemistry (α-SMA) staining of pulmonary arteries in each group. (B) Representative images of H&E and Masson staining of right atrium in each group. (C) CVF of pulmonary artery in each group. (D) CVF of right atrium in each group. (E) α-SMA positive area of pulmonary artery in each group. Data are presented as mean ± standard error of the mean (SEM). *$P < 0.05$, **$P < 0.01$, ***$P < 0.001$, ****$P < 0.0001$. The groups without statistical difference were not labelled. CTL, control; CVF, collagen volume fraction; DAPA, dapagliflozin; H&E, haematoxylin–eosin; MCT, monocrotaline; α-SMA, alpha-smooth muscle actin.

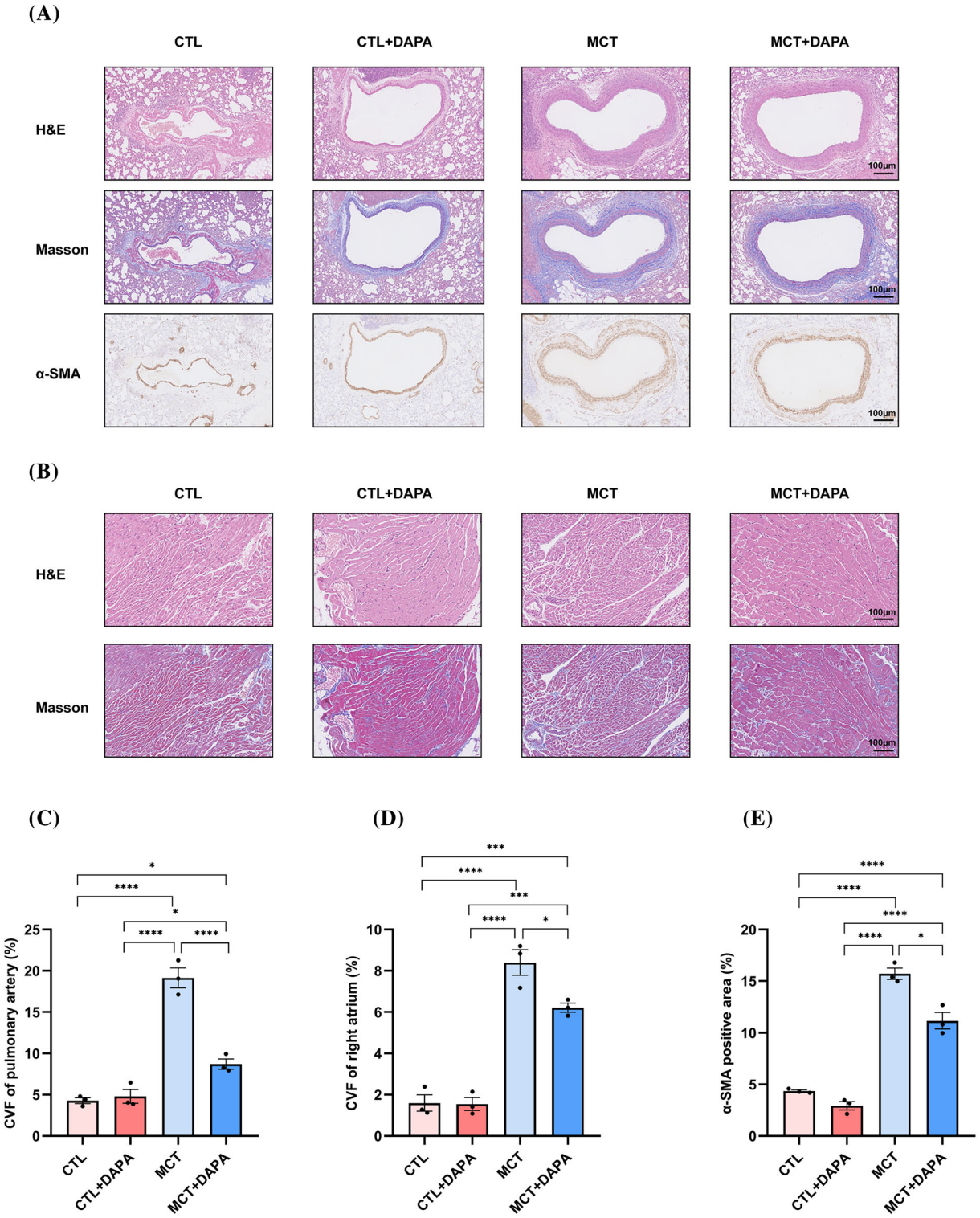

DOI: 10.1002/ehf2.14169

Figure 4 Dapagliflozin can alleviate cardiac electrical remodelling and reduce susceptibility to AF induced by secondary right heart dysfunction. (A) Surface electrocardiogram in each group. (B–I) Trace of P-wave duration, P-wave amplitude, QRS duration, T-wave amplitude, Tpeak-Tend interval, RR interval, PR interval, and QTc interval in surface electrocardiogram in each group (n = 7). (J) Atrial APD_{90} in each group. (K) Atrial ERPs in each group. (L) Inducibility rate of AF in each group. (M) Duration of AF in each group. (N) Representative electrograms of AF induction after atrial burst pacing in isolated perfused heart using Langendorff apparatus. (O) Western blot of the cardiac ion channel- and calmodulin-related proteins in each group (n = 3). Data are presented as mean ± standard error of the mean (SEM). For (I) and (J): $^{*}P < 0.05$, $^{**}P < 0.01$, $^{***}P < 0.001$, $^{****}P < 0.0001$; for (L): $^{*}P < 0.05$ vs. CTL group, $^{\#}P < 0.05$ vs. MCT group. The groups without statistical difference were not labelled. AF, atrial fibrillation; APD_{90}, 90% action potential duration; CTL, control; DAPA, dapagliflozin; ERPs, effective refractory periods; MCT, monocrotaline; NO, no AF occurred; NSR, normal sinus rhythm; QTc, corrected QT.

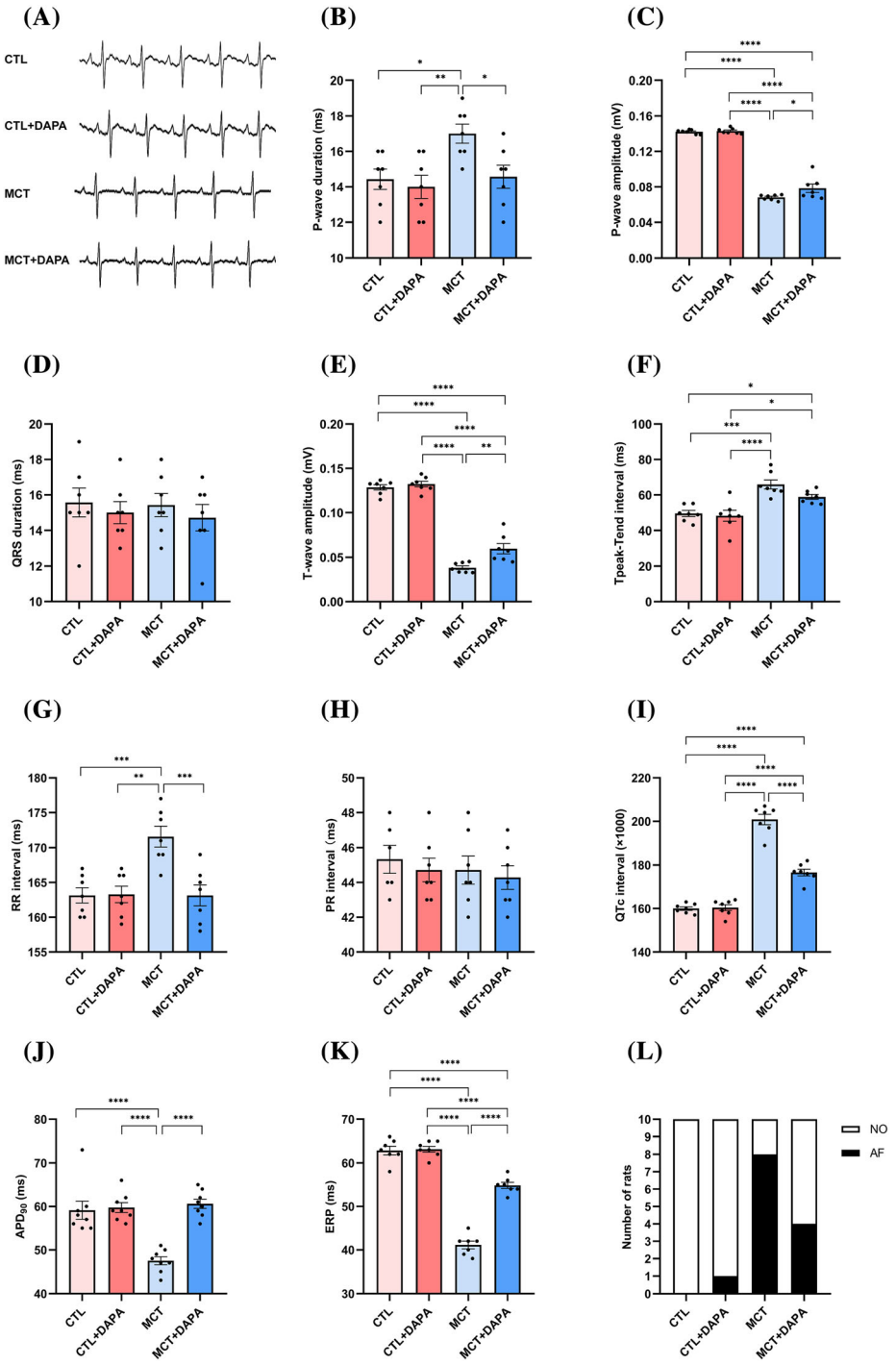

Figure 4 Continued

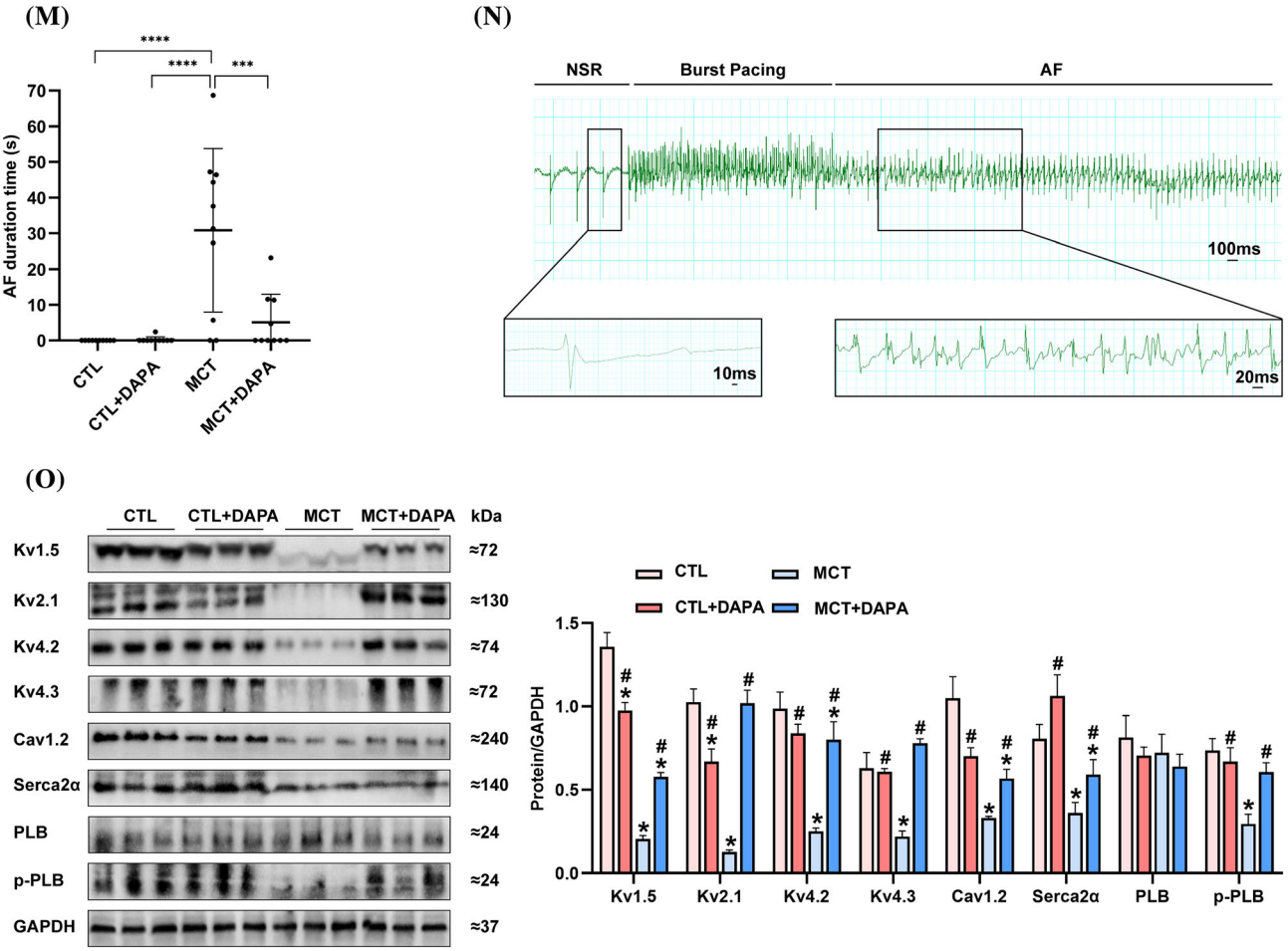

CTL group; 160.40 ± 1.36 ms in the CTL + DAPA group; 176.6 ± 1.57 ms in the MCT + DAPA group; $P < 0.01$) were prolonged in the MCT group, whereas P-wave amplitude (0.07 ± 0.0011 mV, vs. 0.14 ± 0.0009 mV in the CTL group; 0.14 ± 0.0011 mV in the CTL + DAPA group; 0.08 ± 0.0047 mV in the MCT + DAPA group; $P < 0.05$) was decreased, but in the MCT + DAPA group, these changes could partially or completely recover to the level of the CTL group (*Figure 4B,C,G–I*). There was no significant difference in QRS duration and PR interval among groups (*Figure 4D,H*).

In addition to the surface electrocardiographic parameters, we also collected electrophysiological data of isolated heart. Langendorff-perfused hearts were used to characterize changes in electrophysiological parameters: atrial 90% action potential duration (APD_{90}), atrial effective refractory periods (ERPs), inducibility rate of AF, and duration of AF (*Figure 4J–N*). The atrial APD_{90} (47.50 ± 0.93 ms, vs. 59.13 ± 2.1 ms in the CTL group; 59.75 ± 1.13 ms in the CTL + DAPA group; 60.63 ± 1.07 ms in the MCT + DAPA group; $P < 0.01$) and atrial ERPs (41.14 ± 0.88 ms, vs. 62.86 ± 0.99 ms in the CTL group; 63.14 ± 0.67 ms in the CTL + DAPA group; 54.86 ± 0.70 ms in the MCT + DAPA group; $P < 0.01$) of rats in the MCT group were significantly shorter than those in the other groups, and the shortening of these electrophysiological parameters could be partially prolonged in the MCT + DAPA group. Most importantly, the inducibility rate of AF (80%, vs. 0% in the CTL group; 10% in the CTL + DAPA group; 40% in the MCT + DAPA group; $P < 0.05$) and duration of AF (30.85 ± 22.90 s, vs. 0 ± 0 s in the CTL group; 0.24 ± 0.76 s in the CTL + DAPA group; 5.08 ± 7.92 s in the MCT + DAPA group; $P < 0.05$) in the MCT group were significantly higher than those in the other groups, with an inducibility rate of up to 80% and an average duration of 30.85 ± 22.90 s. Both the inducibility rate and duration of AF were significantly declined with the treatment of dapagliflozin (MCT + DAPA group). Meanwhile, the protein expres-

sion levels of cardiac ion channels (Kv1.5, Kv2.1, Kv4.2, Kv4.3, and Cav1.2) and calmodulin (CaM) (including PLB, p-PLB, and Serca2α) in atrial tissues were also evaluated (*Figure 4O*). We found that compared with the other groups, the above-mentioned potassium channels and calcium channels, p-PLB and Serca2α, were significantly down-regulated in the MCT group ($P < 0.05$) but presented a relatively less decline in the MCT + DAPA group. In addition, there was no significant difference in protein expression level with the PLB among groups.

Dapagliflozin may play an anti-remodelling role through toll-like receptor 4/nuclear transcription factor-κB/NACHT, LRR, and PYD domain-containing protein 3 pathway

Through the measuring of mRNA and protein expression levels, we found that toll-like receptor 4/nuclear transcription factor-κB/NACHT, LRR, and PYD domain-containing protein 3 (TLR4/NF-κB/NLRP3) pathway was significantly activated in the process of pulmonary vascular remodelling (MCT group) compared with the other groups ($P < 0.05$). More than that, parameters related to fibrosis, hypertrophy, and inflammation—matrix metalloproteinase 2 (MMP2), beta-myosin heavy chain (β-MHC), transforming growth factor-β1 (TGF-β1), and interleukin-1β (IL-1β)—were all significantly up-regulated in the MCT group ($P < 0.05$). Also, the protein expression levels of atrial natriuretic peptide (ANP) that related to cardiac dilatation or cardiac dysfunction increased significantly in the MCT group ($P < 0.01$), indicating that there was concomitant cardiac dysfunction consistent with the previous functional results. Crucially, the protein expression or gene transcription levels of the above-mentioned indicators that reflect the activation of pathways or the degree of inflammation, fibrosis, and cardiac function were significantly decreased compared with the MCT + DAPA group (*Figure 5A,B*).

Figure 5 Dapagliflozin may play an anti-remodelling role through TLR4/NF-κB/NLRP3 pathway ($n = 3$). (A) Western blot of the pathway-related proteins and hypertrophy/fibrosis/inflammation-related proteins in each group. (B) Relative mRNA levels of the pathway-related genes and hypertrophy/fibrosis/inflammation-related genes in each group. Data are presented as mean ± standard error of the mean (SEM). *$P < 0.05$ vs. CTL group, #$P < 0.05$ vs. MCT group. ANP, atrial natriuretic peptide; CTL, control; DAPA, dapagliflozin; IL-1β, interleukin-1β; MCT, monocrotaline; MMP2, matrix metalloproteinase 2; NF-κB, nuclear transcription factor-κB; NLRP3, NACHT, LRR, and PYD domain-containing protein 3; p-NF-κB, phospho-NF-κB; TGF-β1, transforming growth factor-β1; TLR4, toll-like receptor 4; β-MHC, beta-myosin heavy chain.

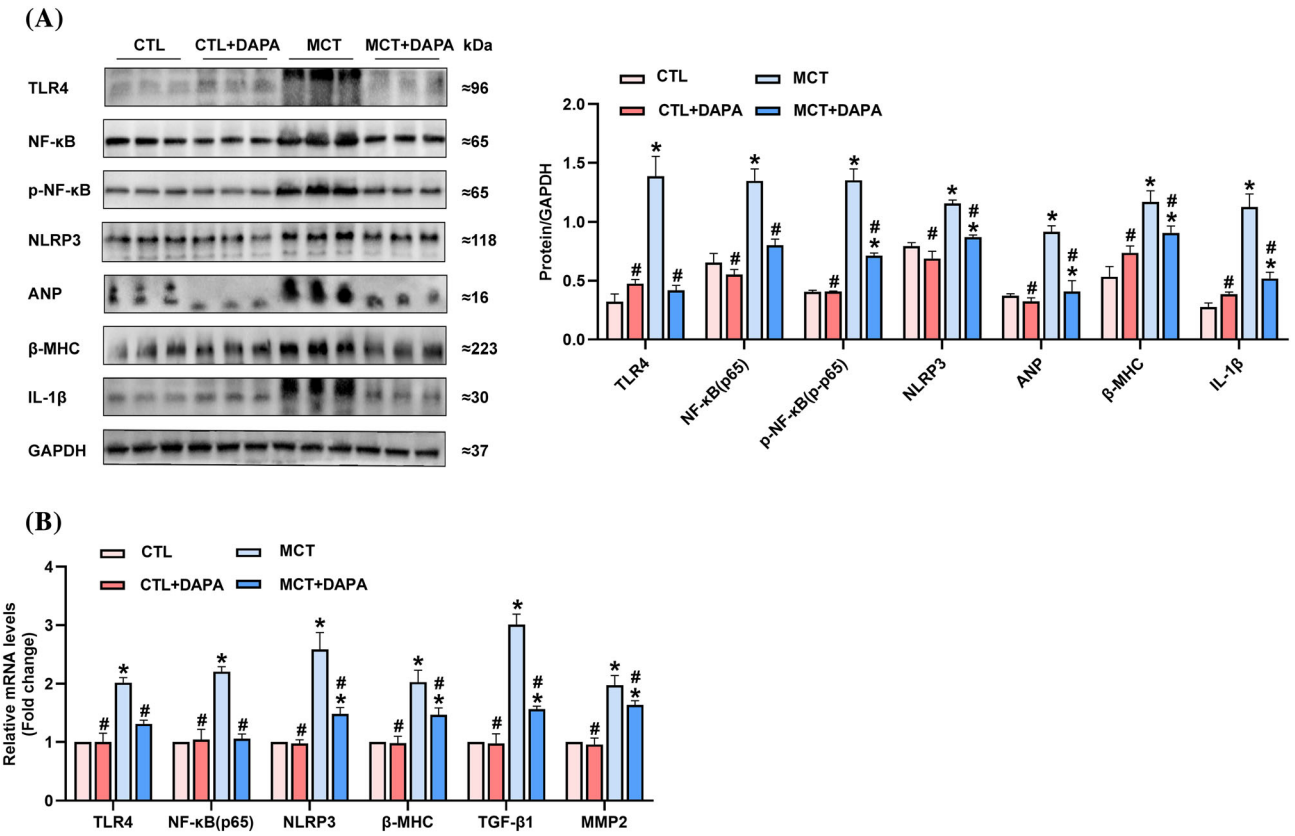

Discussion

MCT is known as pyrrolizidine alkaloid, and pulmonary vascular endothelial cells are considered to be the target cells for its toxic effects. MCT can be converted into active product by cytochrome P450 monooxygenase enzymes in the liver and then transported to the lungs through the blood circulation, causing irreversible pulmonary vascular damage. In addition, it can also promote the formation of pulmonary vascular thrombosis and the proliferation of smooth muscle cells, resulting in muscularization of pulmonary artery and reconstruction of pulmonary vascular structure. Then, all of these pulmonary changes developed into PAH and eventually lead to pulmonary heart disease.[22] According to the toxicological effects of MCT, within 28 days after MCT injection, pulmonary arterial endothelial cells usually appeared swollen, degenerated, necrotic, and exfoliated under the targeted damage of MCT, followed by rupture and accumulation of elastic membrane, enhancement of pulmonary artery muscularization, and perivascular inflammatory response, which will eventually lead to the elevation of pulmonary arterial pressure.[23] Along with that is a significant increase in right heart afterload and a gradual progression to secondary right heart dysfunction. Studies have confirmed that SGLT2is can significantly reduce the risk of cardiovascular disease in patients with high risk of cardiovascular events, especially in patients with cardiac dysfunction.[24–26] In our research, the HW/TL ratio and RVHI, which originally increased due to right heart hypertrophy in secondary right heart dysfunction (MCT group), decreased after treatment with dapagliflozin (MCT + DAPA group). This is consistent with the results of histopathological studies that pulmonary vascular stenosis, atrial collagen deposition, atrial fibrosis, and inflammatory cell aggregation were all improved in the MCT + DAPA group compared with the MCT group. Considering it is clear that dapagliflozin can indeed improve pulmonary vascular remodelling, it is reasonable that it also has therapeutic effect on structural remodelling of right cardiac system. Related results of echocardiography, atrial H&E staining, and Masson staining also supported the antagonistic effect of dapagliflozin on right atrial structural remodelling; that is, dapagliflozin significantly alleviated right heart dysfunction, inflammatory infiltration, and atrial myocardial fibrosis in the MCT + DAPA group compared with the MCT group.

Previous studies have confirmed that myocardial fibrosis and inflammatory infiltration were important factors in the initiation of AF, and the severity of arrhythmia was positively correlated with the deterioration of pathological process and the increase of fibrosis range.[27,28] In addition, it is well known that cardiac dysfunction, especially HF, is closely associated with AF in pathophysiology. Cardiac dysfunction will cause neuroendocrine, structural, and electrophysiological changes in atrium, which can initiate and perpetuate AF. AF can also lead to cardiac structural changes and haemodynamic disorders, which can cause or even worsen cardiac dysfunction. The two often tend to coexist and promote each other in a vicious circle.

In terms of haemodynamics, SGLT2is may affect blood pressure through the following two aspects. On the one hand, one of the side effects of SGLT2is is osmotic diuresis. Because glucose needs to be excreted through urine under the effect of SGLT2is, it will lead to the reduction of blood volume and the contraction of plasma volume. Many studies have reported adverse events such as dehydration, hypovolaemia, postural hypotension, and hypotension associated with oral use of SGLT2is.[29–31] On the other hand, research also found that different from the renal efferent vasodilation caused by renin–angiotensin–aldosterone system (RAAS) inhibitors, SGLT2is would attenuate hyperfiltration through the afferent vasoconstriction mediated by tubuloglomerular feedback, so as to exert a renin–angiotensin system (RAS) inhibition-like effect.[32,33] Therefore, the decrease of blood pressure in the CTL + DAPA group may be related to the above reasons. As for the MCT group, the decrease of blood pressure may be attributed to the following three aspects. Firstly, because the left and right sides of the heart share a septum, the increase in volume and pressure of the right heart caused by PAH will lead to the mechanical septum shift to the left, resulting in geometric, structural, and functional impairment of the left heart. Secondly, the increase of right heart afterload caused by PAH will lead to the obstruction of systemic circulation, resulting in the decrease of effective circulating blood volume and left cardiac output. Along with the reduction of left heart workload and chronic underutilization of left ventricle (LV), the LV will eventually develop into deconditioning and atrophic remodelling, which are characterized by the decrease of LV end-diastolic volume, LV mass, LV systolic strain, stroke volume, and ejection fraction. Finally, either anatomical compression of the left coronary artery by dilated pulmonary artery or inadequate cardiac oxygen and blood supply due to PAH-induced right HF can lead to myocardial ischaemia and hypoxia in the LV, ultimately reducing left ventricular contractility.[34,35] Therefore, there was also a decrease in blood pressure in the MCT group. Interestingly, our results suggested that the MCT + DAPA group appears to have achieved a more positive therapeutic balance in the interaction of these two potential mechanisms and effects.

In terms of cardiac electrophysiology, in this research, after 4 week histopathological changes of right heart and the development of right heart dysfunction in the MCT group, we observed that various electrophysiological parameters, including atrial APD_{90} and ERPs, as well as QTc interval of surface electrocardiogram were changed (the first two were shortened and the last one was prolonged). Most importantly, the inducibility rate of AF increased significantly to 80% compared with the CTL group, which strongly suggested that myocardial fibrosis, inflammatory infiltration, and right heart dysfunction due to increased afterload were risk factors for the initiation

DOI: 10.1002/ehf2.14169

of AF. Besides, the surface electrocardiographic results are also consistent with recent research that QTc interval prolongation can be a strong and effective predictor of AF induced by a variety of diseases.[36–38] Importantly, it is worth mentioning that the potassium and calcium ion channels and CaM in atrial tissues also underwent ion channel remodelling in the process of histopathological and functional changes. These abnormal electrophysiological changes were significantly improved in the MCT + DAPA group, which is likely attributed to dapagliflozin. Many studies have shown that in the model of cardiac hypertrophy or HF, the abnormal protein expression of potassium and calcium channels plays a key role in the change of atrial APD_{90}, ERPs, and QTc interval, and the initiation and perpetuation of AF are also associated with this expression disorder.[39–41] Taken together, clues suggested that the potential molecular mechanism of the anti-atrial arrhythmia effect of dapagliflozin may through the regulation of channel protein remodelling. Besides, previous studies have also found that SGLT2is can improve mitochondrial respiration by reducing accumulation of reactive oxygen species (ROS) and consumption of adenosine triphosphate (ATP).[42] Considering that functional exertion of numerous cardiac ion channels or protein pumps mostly depends on the energy supply of mitochondria, SGLT2is may also affect electromechanical function remodelling from the perspective of regulating mitochondrial energy.

Furthermore, activation of inflammatory response is a key factor in the initiation and perpetuation of AF. NLRP3 inflammasome, as a vital participant in innate immunity and inflammation, has been proved to be involved in the pathophysiological process of AF in both human and animal models, and inhibition of NLRP3 inflammasome or knockout of NLRP3 inflammasome gene can prevent the development of AF.[43–46] The typical function of NLRP3 inflammasome in immune cells such as macrophages, T lymphocytes, or eosinophils/neutrophils is to promote the oligomerization of inflammasome, so as to activate caspase-1 and promote inflammatory cytokines such as IL-1β. This effect is induced by TLR/NF-κB signalling pathway to initiate NLRP3 inflammasome and precursor caspase-1 (pro-CasP1) transcription.[44,47] In recent years, TLR4/NF-κB pathway has been shown to play a role in atrial structural remodelling and inflammation promotion,[17] whereas TLR4/NF-κB/NLRP3 pathway may also be involved in myocardial ischaemia–reperfusion injury and renal protection.[48–50] Activation of this pathway can increase the inflammatory cytokines released by macrophages and other inflammatory cells. Moreover, important elements of this pathway also play a role in PAH.[51] Therefore, we tried to explore this possible pathway. We found that TLR4/NF-κB/NLRP3 may be the regulatory pathway of anti-atrial fibrosis and inflammation. Compared with the CTL group, the protein and mRNA levels of key elements of this pathway in the MCT group were significantly up-regulated, whereas the MCT + DAPA group showed antagonism effect to this pathway. In fact, there are many signalling pathways against inflammation and fibrosis, but dapagliflozin plays a role at least in part through this pathway according to our research results. Through this biological signalling pathway, dapagliflozin can down-regulate inflammation and fibrosis-related IL-1β and TGF-β1, β-MHC, and MMP2, so as to play a preventive role in atrial structural and electrical remodelling secondary right heart dysfunction. Recent studies have suggested that epicardial adipose tissue (EAT) can cause AF through paracrine or vascular endothelial secretion of pro-inflammatory and profibrotic cytokines.[52,53] Most notably, SGLT2is have a selective targeting effect on atrial EAT, which can reduce local atrial inflammation and induce sympathetic neurolysis of atrial EAT.[54,55] Therefore, in this study, in addition to directly reducing the inflammatory and fibrotic response of atrial tissue, whether dapagliflozin also plays a role by improving these effects of EAT is worthy of further study. However, the purpose of this study is to report and preliminarily explore the novel preventive and therapeutic effect of dapagliflozin, and more in-depth mechanism needs to be clarified in the future studies.

Beyond that, the initiation and perpetuation of AF are gradually progressive with the formation of PAH. Once AF is initiated, it will not disappear completely due to the decrease of pulmonary arterial pressure. Indeed, improving pulmonary fibrosis and reducing pulmonary arterial pressure can reduce the susceptibility to AF, but the initiation and perpetuation of AF do not solely rely on this structural and haemodynamic remodelling, and arrhythmia has been considered as a sequela caused by PAH (end-organ injury patterns that develop secondarily to PH–right HF),[56] which also suggests that AF still exists even if pulmonary arterial pressure returns to normal and right heart function is rectified. This is what we called ‘AF begets AF’. Therefore, the net reduction of AF susceptibility observed by dapagliflozin treatment cannot be generally attributed to the effect on pulmonary vascular system alone. Needless to say, dapagliflozin can also reduce systolic blood pressure and body weight, which are risk factors of both HF and AF. Taken together, we simulated the gradual formation of PAH in this research, aiming to convey the research idea as following: Dapagliflozin can reduce the susceptibility to AF during the progression of right heart dysfunction, and the mechanism is likely to be the improvement of PAH and fibrosis, antagonization ion channels’ electrical remodelling, or regulating NLRP3 inflammasome. Each of the possible potential mechanisms exists independently but also influences each other.

Limitations

In this research, we investigated the arrhythmic parameters such as the inducibility rate of AF in the isolated hearts of

rat, which may differ from the real status *in vivo* due to the lack of corresponding influence of the autonomic nervous system. However, the relevant research results are consistent with the trend of clinical phenomena observed in macro clinical practice.

Conclusions

In this research, we observed that dapagliflozin can reduce pulmonary vascular damage and RHD in MCT-exposed rats. In addition, it can also reduce the susceptibility to AF caused by right heart dysfunction secondary to pulmonary vascular remodelling. The underlying mechanism of dapagliflozin in the treatment of atrial structural remodelling may be related to its antagonism effect of fibrosis and NLRP3 inflammasome-associated inflammatory pathway, whereas its mechanism in the treatment of atrial electrical remodelling may be related to the antagonism of ion channel remodelling. In summary, in addition to its ground-breaking efficacy in the field of HF, dapagliflozin may also have a potential preventive and therapeutic value in RHD-induced AF.

Conflicts of interest

The authors declare that they have no known competing financial interests or personal relationships that could have appeared to influence the work reported in this paper.

Funding

This work was supported by grants from the National Natural Science Foundation of China (No. 82070330) and the Fundamental Research Funds for the Central Universities (No. 2042021kf0119).

Supporting information

Additional supporting information may be found online in the Supporting Information section at the end of the article.

Appendix S1. Supplementary data

References

1. Braunwald E. SGLT2 inhibitors: the statins of the 21st century. *Eur Heart J*. 2021; **43**: 1029–1030.
2. McMurray JJV, DeMets DL, Inzucchi SE, Køber L, Kosiborod MN, Langkilde AM, Martinez FA, Bengtsson O, Ponikowski P, Sabatine MS, Sjöstrand M, Solomon SD, DAPA-HF Committees and Investigators. The Dapagliflozin And Prevention of Adverse-outcomes in Heart Failure (DAPA-HF) trial: baseline characteristics. *Eur J Heart Fail*. 2019; **21**: 1402–1411.
3. Martinez FA, Serenelli M, Nicolau JC, Petrie MC, Chiang CE, Tereshchenko S, Solomon SD, Inzucchi SE, Kober L, Kosiborod MN, Ponikowski P, Sabatine MS, DeMets DL, Dutkiewicz-Piasecka M, Bengtsson O, Sjostrand M, Langkilde AM, Jhund PS, McMurray JJV. Efficacy and safety of dapagliflozin in heart failure with reduced ejection fraction according to age: insights from DAPA-HF. *Circulation*. 2020; **141**: 100–111.
4. Kosiborod MN, Jhund PS, Docherty KF, Diez M, Petrie MC, Verma S, Nicolau JC, Merkely B, Kitakaze M, DeMets DL, Inzucchi SE, Kober L, Martinez FA, Ponikowski P, Sabatine MS, Solomon SD, Bengtsson O, Lindholm D, Niklasson A, Sjostrand M, Langkilde AM, McMurray JJV. Effects of dapagliflozin on symptoms, function, and quality of life in patients with heart failure and reduced ejection fraction: results from the DAPA-HF trial. *Circulation*. 2020; **141**: 90–99.
5. Jhund PS, Solomon SD, Docherty KF, Heerspink HJL, Anand IS, Bohm M, Chopra V, de Boer RA, Desai AS, Ge J, Kitakaze M, Merkley B, O'Meara E, Shou M, Tereshchenko S, Verma S, Vinh PN, Inzucchi SE, Kober L, Kosiborod MN, Martinez FA, Ponikowski P, Sabatine MS, Bengtsson O, Langkilde AM, Sjostrand M, McMurray JJV. Efficacy of dapagliflozin on renal function and outcomes in patients with heart failure with reduced ejection fraction: results of DAPA-HF. *Circulation*. 2021; **143**: 298–309.
6. O'Meara E, McDonald M, Chan M, Ducharme A, Ezekowitz JA, Giannetti N, Grzeslo A, Heckman GA, Howlett JG, Koshman SL, Lepage S, Mielniczuk LM, Moe GW, Swiggum E, Toma M, Virani SA, Zieroth S, De S, Matteau S, Parent MC, Asgar AW, Cohen G, Fine N, Davis M, Verma S, Cherney D, Abrams H, Al-Hesayen A, Cohen-Solal A, D'Astous M, Delgado DH, Desplantie O, Estrella-Holder E, Green L, Haddad H, Harkness K, Hernandez AF, Kouz S, LeBlanc MH, Lee D, Masoudi FA, McKelvie RS, Rajda M, Ross HJ, Sussex B. CCS/CHFS heart failure guidelines: clinical trial update on functional mitral regurgitation, SGLT2 inhibitors, ARNI in HFpEF, and tafamidis in amyloidosis. *Can J Cardiol*. 2020; **36**: 159–169.
7. Li HL, Lip GH, Feng Q, Fei Y, Tse YK, Wu MZ, Ren QW, Tse HF, Cheung BY, Yiu KH. Sodium-glucose cotransporter 2 inhibitors (SGLT2i) and cardiac arrhythmias: a systematic review and meta-analysis. *Cardiovasc Diabetol*. 2021; **20**: 100.
8. Fernandes GC, Fernandes A, Cardoso R, Penalver J, Knijnik L, Mitrani RD, Myerburg RJ, Goldberger JJ. Association of SGLT2 inhibitors with arrhythmias and sudden cardiac death in patients with type 2 diabetes or heart failure: a meta-analysis of 34 randomized controlled trials. *Heart Rhythm*. 2021; **18**: 1098–1105.
9. Wit AL, Boyden PA. Triggered activity and atrial fibrillation. *Heart Rhythm*. 2007; **4**: S17–S23.
10. Hasebe H, Yoshida K, Iida M, Hatano N, Muramatsu T, Aonuma K. Right-to-left frequency gradient during atrial fibrillation initiated by right atrial ectopies and its augmentation by adenosine triphosphate: implications of right atrial fibrillation. *Heart Rhythm*. 2016; **13**: 354–363.
11. Nademanee K, McKenzie J, Kosar E, Schwab M, Sunsaneewitayakul B, Vasavakul T, Khunnawat C, Ngarmukos T. A new approach for catheter ablation of atrial fibrillation: mapping of the elec-

trophysiologic substrate. *J Am Coll Cardiol*. 2004; **43**: 2044–2053.
12. Rajdev A, Garan H, Biviano A. Arrhythmias in pulmonary arterial hypertension. *Prog Cardiovasc Dis*. 2012; **55**: 180–186.
13. Goudis CA. Chronic obstructive pulmonary disease and atrial fibrillation: an unknown relationship. *J Cardiol*. 2017; **69**: 699–705.
14. Drakopoulou M, Nashat H, Kempny A, Alonso-Gonzalez R, Swan L, Wort SJ, Price LC, McCabe C, Wong T, Gatzoulis MA, Ernst S, Dimopoulos K. Arrhythmias in adult patients with congenital heart disease and pulmonary arterial hypertension. *Heart*. 2018; **104**: 1963–1969.
15. Hiram R, Naud P, Xiong F, Al-U'datt D, Algalarrondo V, Sirois MG, Tanguay JF, Tardif JC, Nattel S. Right atrial mechanisms of atrial fibrillation in a rat model of right heart disease. *J Am Coll Cardiol*. 2019; **74**: 1332–1347.
16. Joannides CN, Mangiafico SP, Waters MF, Lamont BJ, Andrikopoulos S. Dapagliflozin improves insulin resistance and glucose intolerance in a novel transgenic rat model of chronic glucose overproduction and glucose toxicity. *Diabetes Obes Metab*. 2017; **19**: 1135–1146.
17. Shuai W, Kong B, Fu H, Shen C, Jiang X, Huang H. MD1 deficiency promotes inflammatory atrial remodelling induced by high-fat diets. *Can J Cardiol*. 2019; **35**: 208–216.
18. Dai Y, Chen X, Song X, Chen X, Ma W, Lin J, Wu H, Hu X, Zhou Y, Zhang H, Liao Y, Qiu Z, Zhou Z. Immunotherapy of endothelin-1 receptor type A for pulmonary arterial hypertension. *J Am Coll Cardiol*. 2019; **73**: 2567–2580.
19. Greiner S, Jud A, Aurich M, Hess A, Hilbel T, Hardt S, Katus HA, Mereles D. Reliability of noninvasive assessment of systolic pulmonary artery pressure by Doppler echocardiography compared to right heart catheterization: analysis in a large patient population. *J Am Heart Assoc*. 2014; **3**: e001103.
20. Sohrabi B, Kazemi B, Mehryar A, Teimouri-Dereshki A, Toufan M, Aslanabadi N. Correlation between pulmonary artery pressure measured by echocardiography and right heart catheterization in patients with rheumatic mitral valve stenosis (a prospective study). *Echocardiography*. 2016; **33**: 7–13.
21. Schewel J, Schluter M, Schmidt T, Kuck KH, Frerker C, Schewel D. Correlation between Doppler echocardiography and right heart catheterization assessment of systolic pulmonary artery pressure in patients with severe aortic stenosis. *Echocardiography*. 2020; **37**: 380–387.
22. Wilson DW, Segall HJ, Pan LC, Lame MW, Estep JE, Morin D. Mechanisms and pathology of monocrotaline pulmonary toxicity. *Crit Rev Toxicol*. 1992; **22**: 307–325.
23. Schultze AE, Roth RA. Chronic pulmonary hypertension—the monocrotaline model and involvement of the hemostatic system. *J Toxicol Environ Health B Crit Rev*. 1998; **1**: 271–346.
24. Zinman B, Wanner C, Lachin JM, Fitchett D, Bluhmki E, Hantel S, Mattheus M, Devins T, Johansen OE, Woerle HJ, Broedl UC, Inzucchi SE, for the EMPA-REG OUTCOME Investigators. Empagliflozin, cardiovascular outcomes, and mortality in type 2 diabetes. *N Engl J Med*. 2015; **373**: 2117–2128.
25. Verma S, Dhingra NK, Butler J, Anker SD, Ferreira JP, Filippatos G, Januzzi JL, Lam CSP, Sattar N, Peil B, Nordaby M, Brueckmann M, Pocock SJ, Zannad F, Packer M, EMPEROR-Reduced trial committees and investigators. Empagliflozin in the treatment of heart failure with reduced ejection fraction in addition to background therapies and therapeutic combinations (EMPEROR-Reduced): a post-hoc analysis of a randomised, double-blind trial. *Lancet Diabetes Endocrinol*. 2021; **10**: 35–45.
26. Jhund PS, Ponikowski P, Docherty KF, Gasparyan SB, Bohm M, Chiang CE, Desai AS, Howlett J, Kitakaze M, Petrie MC, Verma S, Bengtsson O, Langkilde AM, Sjostrand M, Inzucchi SE, Kober L, Kosiborod MN, Martinez FA, Sabatine MS, Solomon SD, McMurray JJV. Dapagliflozin and recurrent heart failure hospitalizations in heart failure with reduced ejection fraction: an analysis of DAPA-HF. *Circulation*. 2021; **143**: 1962–1972.
27. Nattel S, Heijman J, Zhou L, Dobrev D. Molecular basis of atrial fibrillation pathophysiology and therapy: a translational perspective. *Circ Res*. 2020; **127**: 51–72.
28. Luscher TF. Challenges in atrial fibrillation: detection, alert systems, fibrosis, and infection. *Eur Heart J*. 2020; **41**: 1063–1066.
29. Wiviott SD, Raz I, Bonaca MP, Mosenzon O, Kato ET, Cahn A, Silverman MG, Zelniker TA, Kuder JF, Murphy SA, Bhatt DL, Leiter LA, McGuire DK, Wilding JPH, Ruff CT, Gause-Nilsson IAM, Fredriksson M, Johansson PA, Langkilde AM, Sabatine MS, Investigators D-T. Dapagliflozin and cardiovascular outcomes in type 2 diabetes. *N Engl J Med*. 2019; **380**: 347–357.
30. Scheen AJ. Pharmacodynamics, efficacy and safety of sodium-glucose co-transporter type 2 (SGLT2) inhibitors for the treatment of type 2 diabetes mellitus. *Drugs*. 2015; **75**: 33–59.
31. Salah HM, Al'Aref SJ, Khan MS, Al-Hawwas M, Vallurupalli S, Mehta JL, Mounsey JP, Greene SJ, McGuire DK, Lopes RD, Fudim M. Efficacy and safety of sodium-glucose cotransporter 2 inhibitors initiation in patients with acute heart failure, with and without type 2 diabetes: a systematic review and meta-analysis. *Cardiovasc Diabetol*. 2022; **21**: 20.
32. Petrykiv S, Laverman GD, de Zeeuw D, Heerspink HJL. Does SGLT2 inhibition with dapagliflozin overcome individual therapy resistance to RAAS inhibition? *Diabetes Obes Metab*. 2018; **20**: 224–227.
33. Cherney DZ, Perkins BA, Soleymanlou N, Xiao F, Zimpelmann J, Woerle HJ, Johansen OE, Broedl UC, von Eynatten M, Burns KD. Sodium glucose cotransport-2 inhibition and intrarenal RAS activity in people with type 1 diabetes. *Kidney Int*. 2014; **86**: 1057–1058.
34. Rosenkranz S, Howard LS, Gomberg-Maitland M, Hoeper MM. Systemic consequences of pulmonary hypertension and right-sided heart failure. *Circulation*. 2020; **141**: 678–693.
35. Naeije R, Richter MJ, Rubin LJ. The physiologic basis of pulmonary arterial hypertension. *Eur Respir J*. 2021; **59**: 2102334.
36. Zhang N, Gong M, Tse G, Zhang Z, Meng L, Yan BP, Zhang L, Wu G, Xia Y, Xin-Yan G, Li G, Liu T. Prolonged corrected QT interval in predicting atrial fibrillation: a systematic review and meta-analysis. *Pacing Clin Electrophysiol*. 2018; **41**: 321–327.
37. Roberts JD, Soliman EZ, Alonso A, Vittinghoff E, Chen LY, Loehr L, Marcus GM. Electrocardiographic intervals associated with incident atrial fibrillation: dissecting the QT interval. *Heart Rhythm*. 2017; **14**: 654–660.
38. Hoshino T, Nagao T, Shiga T, Maruyama K, Toi S, Mizuno S, Ishizuka K, Shimizu S, Uchiyama S, Kitagawa K. Prolonged QTc interval predicts poststroke paroxysmal atrial fibrillation. *Stroke*. 2015; **46**: 71–76.
39. Liu W, Wang G, Zhang C, Ding W, Cheng W, Luo Y, Wei C, Liu J. MG53, a novel regulator of KChIP2 and $I_{to,f}$, plays a critical role in electrophysiological remodeling in cardiac hypertrophy. *Circulation*. 2019; **139**: 2142–2156.
40. Burg S, Attali B. Targeting of potassium channels in cardiac arrhythmias. *Trends Pharmacol Sci*. 2021; **42**: 491–506.
41. Narayan SM, Franz MR, Clopton P, Pruvot EJ, Krummen DE. Repolarization alternans reveals vulnerability to human atrial fibrillation. *Circulation*. 2011; **123**: 2922–2930.
42. Okunrintemi V, Mishriky BM, Powell JR, Cummings DM. Sodium-glucose co-transporter-2 inhibitors and atrial fibrillation in the cardiovascular and renal outcome trials. *Diabetes Obes Metab*. 2021; **23**: 276–280.
43. Yao C, Veleva T, Scott L Jr, Cao S, Li L, Chen G, Jeyabal P, Pan X, Alsina KM, Abu-Taha ID, Ghezelbash S, Reynolds CL, Shen YH, LeMaire SA, Schmitz W, Muller FU, El-Armouche A, Tony Eissa N, Beeton C, Nattel S, Wehrens XHT, Dobrev D, Li N. Enhanced cardiomyocyte NLRP3 inflammasome signaling promotes atrial fibrillation. *Circulation*. 2018; **138**: 2227–2242.
44. Li N, Brundel B. Inflammasomes and proteostasis novel molecular mechanisms associated with atrial fibrillation. *Circ Res*. 2020; **127**: 73–90.

45. Scott L Jr, Fender AC, Saljic A, Li L, Chen X, Wang X, Linz D, Lang J, Hohl M, Twomey D, Pham TT, Diaz-Lankenau R, Chelu MG, Kamler M, Entman ML, Taffet GE, Sanders P, Dobrev D, Li N. NLRP3 inflammasome is a key driver of obesity-induced atrial arrhythmias. *Cardiovasc Res*. 2021; **117**: 1746–1759.
46. Heijman J, Muna AP, Veleva T, Molina CE, Sutanto H, Tekook M, Wang Q, Abu-Taha IH, Gorka M, Kunzel S, El-Armouche A, Reichenspurner H, Kamler M, Nikolaev V, Ravens U, Li N, Nattel S, Wehrens XHT, Dobrev D. Atrial myocyte NLRP3/CaMKII nexus forms a substrate for postoperative atrial fibrillation. *Circ Res*. 2020; **127**: 1036–1055.
47. Lamkanfi M, Dixit VM. Inflammasomes and their roles in health and disease. *Annu Rev Cell Dev Biol*. 2012; **28**: 137–161.
48. Zhang X, Du Q, Yang Y, Wang J, Dou S, Liu C, Duan J. The protective effect of Luteolin on myocardial ischemia/reperfusion (I/R) injury through TLR4/NF-κB/NLRP3 inflammasome pathway. *Biomed Pharmacother*. 2017; **91**: 1042–1052.
49. Gao H, Wang X, Qu X, Zhai J, Tao L, Zhang Y, Song Y, Zhang W. Omeprazole attenuates cisplatin-induced kidney injury through suppression of the TLR4/NF-κB/NLRP3 signaling pathway. *Toxicology*. 2020; **440**: 152487.
50. Dai Y, Wang S, Chang S, Ren D, Shali S, Li C, Yang H, Huang Z, Ge J. M2 macrophage-derived exosomes carry microRNA-148a to alleviate myocardial ischemia/reperfusion injury via inhibiting TXNIP and the TLR4/NF-κB/NLRP3 inflammasome signaling pathway. *J Mol Cell Cardiol*. 2020; **142**: 65–79.
51. Cero FT, Hillestad V, Sjaastad I, Yndestad A, Aukrust P, Ranheim T, Lunde IG, Olsen MB, Lien E, Zhang L, Haugstad SB, Loberg EM, Christensen G, Larsen KO, Skjonsberg OH. Absence of the inflammasome adaptor ASC reduces hypoxia-induced pulmonary hypertension in mice. *Am J Physiol Lung Cell Mol Physiol*. 2015; **309**: L378–L387.
52. Packer M. Disease-treatment interactions in the management of patients with obesity and diabetes who have atrial fibrillation: the potential mediating influence of epicardial adipose tissue. *Cardiovasc Diabetol*. 2019; **18**: 121.
53. Batal O, Schoenhagen P, Shao M, Ayyad AE, Van Wagoner DR, Halliburton SS, Tchou PJ, Chung MK. Left atrial epicardial adiposity and atrial fibrillation. *Circ Arrhythm Electrophysiol*. 2010; **3**: 230–236.
54. Iacobellis G. Epicardial adipose tissue in contemporary cardiology. *Nat Rev Cardiol*. 2022; **19**: 593–606.
55. Artola Arita V, Van Veldhuisen DJ, Rienstra M. Dapagliflozin effect on heart failure with prevalent or new-onset atrial fibrillation. *Eur J Heart Fail*. 2022; **24**: 526–528.
56. Maron BA, Abman SH, Elliott CG, Frantz RP, Hopper RK, Horn EM, Nicolls MR, Shlobin OA, Shah SJ, Kovacs G, Olschewski H, Rosenzweig EB. Pulmonary arterial hypertension: diagnosis, treatment, and novel advances. *Am J Respir Crit Care Med*. 2021; **203**: 1472–1487.